

BRIEF REPORT

Open Access



Expanding the phenotype associated with biallelic *SCNM1* variants

Asier Iturrate^{1,2}, Frédéric Tran-Mau Them^{3,4}, Alain Verloes⁵, Antoine Pouzet⁵, Deepthi de Silva⁶, Laurence Perrin-Sabourin⁵, Ingrid M. Wentzensen⁷, Kennedy Jones⁸, Jariya Upadia⁸, Ebtessam Abdalla⁹, Christel Thauvin-Robinet^{3,4,10}, Victor L. Ruiz-Perez^{1,2,11*} and Ange-Line Bruel^{3,4*}

Abstract

Background Oral-facial-digital (OFD) syndrome comprises a number of genetically and clinically heterogeneous ciliopathies characterized by distinctive craniofacial, oral cavity and extremities abnormalities. Recently, *SCNM1*, encoding a protein component of the minor spliceosome, was associated with OFD syndrome. Until now, only three families had been described with pathogenic variants in this gene.

Results Using exome sequencing, we identified biallelic variants in *SCNM1* in five additional patients diagnosed with OFD syndrome from four unrelated families. Clinical evaluation of these patients revealed novel features linked to *SCNM1* including neurodevelopmental disorders, oculomotor apraxia and skeletal abnormalities. The pathogenicity of a missense variant affecting the C2H2 zinc finger domain of *SCNM1*, p.(His68Arg), was verified in fibroblasts from a patient with this variant in the homozygous state. These cells exhibited comparable defects to those previously reported in cells lacking *SCNM1*, including diminished expression of several U12-intron containing genes such as *TMEM107* and *CIBAR1*, two ciliary genes previously associated with OFD syndrome and postaxial polydactyly, respectively, and abnormal primary cilia. In addition, the mutant version of *SCNM1* harboring the p.(His68Arg) change was unable to rescue the phenotype of *SCNM1*-deficient cells.

Conclusions This work expands the molecular and clinical landscape of the *SCNM1*-related condition and shows that pathogenic variants in this gene cause a complex phenotype overlapping with OFD types II and VI. Our data improves understanding of the ciliopathy linked to *SCNM1*, which is of paramount importance in terms of genetic counselling, particularly with regard to the risks associated with neurodevelopmental disorders.

Keywords *SCNM1*, Orofaciodigital syndrome, Primary cilia, Minor spliceosome, U12-intron

*Correspondence:
Victor L. Ruiz-Perez
vlruiz@iib.uam.es
Ange-Line Bruel
ange-line.brue@u-bourgogne.fr

Full list of author information is available at the end of the article



© The Author(s) 2025. **Open Access** This article is licensed under a Creative Commons Attribution-NonCommercial-NoDerivatives 4.0 International License, which permits any non-commercial use, sharing, distribution and reproduction in any medium or format, as long as you give appropriate credit to the original author(s) and the source, provide a link to the Creative Commons licence, and indicate if you modified the licensed material. You do not have permission under this licence to share adapted material derived from this article or parts of it. The images or other third party material in this article are included in the article's Creative Commons licence, unless indicated otherwise in a credit line to the material. If material is not included in the article's Creative Commons licence and your intended use is not permitted by statutory regulation or exceeds the permitted use, you will need to obtain permission directly from the copyright holder. To view a copy of this licence, visit <http://creativecommons.org/licenses/by-nc-nd/4.0/>.

Background

Oral-facial-digital (OFD) syndrome represents a heterogeneous group of ciliopathies which are distinguished by the association of craniofacial (hypertelorism, cleft lip, micro or macrocephaly), oral cavity (hamartomas, lobulated tongue, cleft palate) and extremities abnormalities (polydactyly, brachydactyly). Patients may also have a wide range of additional features such as neurodevelopmental disorders, polycystic kidney disease, cerebral, musculoskeletal or cardiac malformations, and obesity, that delineate a growing list of OFD syndrome subtypes [1]. The most frequent form, OFD I [MIM # 311200], is caused by pathogenic variants in the *OFD1* gene [2], and is characterized by typical oral, facial, and digital findings, polycystic kidney disease, milia, and brain MRI findings, including agenesis of the corpus callosum with or without Dandy-Walker malformation. Intellectual disability is reported in half of the cases. The other frequently described OFD sub-type is OFD VI [MIM # 277170], which is mainly featured by molar tooth sign, cardiac malformations and deafness. Genes responsible for OFD VI are *C5orf42*, *TMEM107*, *TMEM138*, *TMEM216* and *TMEM231* [1]. Other rare or ultra-rare OFD subtypes are defined by the clinical specificity of their phenotype. For example, OFD II [MIM # 252100] is characterized by short stature, hearing loss and normal intelligence, OFD IV [MIM # 258860] by short tibiae, and OFD XIV [MIM # 615948] by severe microcephaly and intellectual disability. In total, more than 30 genes encoding ciliary proteins or proteins involved in primary cilia formation have been associated with OFD syndrome [3]. Typically, the inheritance pattern of this condition is autosomal recessive, except for the *OFD1* and *ZRSR2*-related OFD types, which have a dominant or recessive X-linked inheritance, respectively.

Ciliopathies are a family of related disorders arising from the dysfunction or absence of primary cilia. These cellular organelles are microtubule-based structures projecting from the cytoplasmic membrane that are involved in a variety of sensory processes, being particularly essential in development. Primary cilia are enriched in receptors and ion channels that sense photo, chemo and mechanical stimuli and facilitate the transduction of key signaling pathways [1]. There are five major structural regions related to primary cilia: (1) the centrosome, (2) the basal body, which initiates cilium assembly; (3) the transition zone, placed at the distal end of the basal body; (4) the transition fibers, that create a diffusion barrier to regulate protein content in the ciliary compartment; and (5) the axonemal microtubules.

Recently, bi-allelic loss-of-function variants in *SCNMI* were identified in three unrelated consanguineous families (4 affected patients) presenting with OFD syndrome. This first report of patients with pathogenic variants in

SCNMI suggested a phenotype linked to this gene similar to OFD type II syndrome, including lobulated tongue with nodules, hypodontia, high palate, broad nasal bridge, downturned corners of mouth, median notching of lip, retrognathia, short arm and tibiae, brachy and polysyndactyly, but not psychomotor or cognitive retardation [3].

SCNMI encodes a protein component of the minor spliceosome, which is a ribonucleoprotein complex responsible for excising a specific group of introns known as U12-type introns or minor introns. U12-type introns have divergent and highly conserved 5' splice site and branch point sequences, and are present in around 700–800 human genes [4]. *SCNMI* null cells were described having a significant increase in U12-type intron retention and aberrant splicing of targeted transcripts including ciliary genes such as *TMEM107* (OFD syndrome, [MIM # 617563]) and *CIBARI* (Polydactyly, postaxial, type A9, [MIM # 618219]). Furthermore, cilia defects were shown to emerge in the absence *SCNMI* [3].

Herein, we report five new patients from four unrelated families with bi-allelic variants in *SCNMI* and a clinical phenotype of OFD syndrome. The identification of additional clinical features in these patients suggests a broader and more complex phenotypic spectrum, ranging from OFD syndrome type II to type VI.

Materials and methods

Material and Methods of this article are provided as supplementary information.

Results

Clinical assessment

Family I: Affected individuals from family I, patients 1 (P1) and 2 (P2), are siblings born to first-cousin parents originally from Afghanistan who also have 5 healthy children. P1 is a teenager for whom there are no records about birth and infancy. Maternal history, pregnancy, birth and childhood are not documented. At the age of 14 years, during the first documented examination, he was overweight (+2SD), with normal height and occipital-frontal parameter measurements. He presented a right eye cataract, low-set ears, high palate and hamartoma of the tongue. Extremities showed suspected polydactyly, because of very broad first phalanges of fingers and toes, and syndactyly which was surgically corrected in Afghanistan. There was no X-ray examination to confirm skeletal defects. He also had a bilateral equinovarus deformity causing gait disturbances. Cardiac, hepatic, renal and gastrointestinal investigations revealed no additional defects and brain MRI was normal. Neurodevelopmental features identified at 14 years of age included a history of global developmental delay, psychomotor delay, and suspected speech delay with limited use of sentences

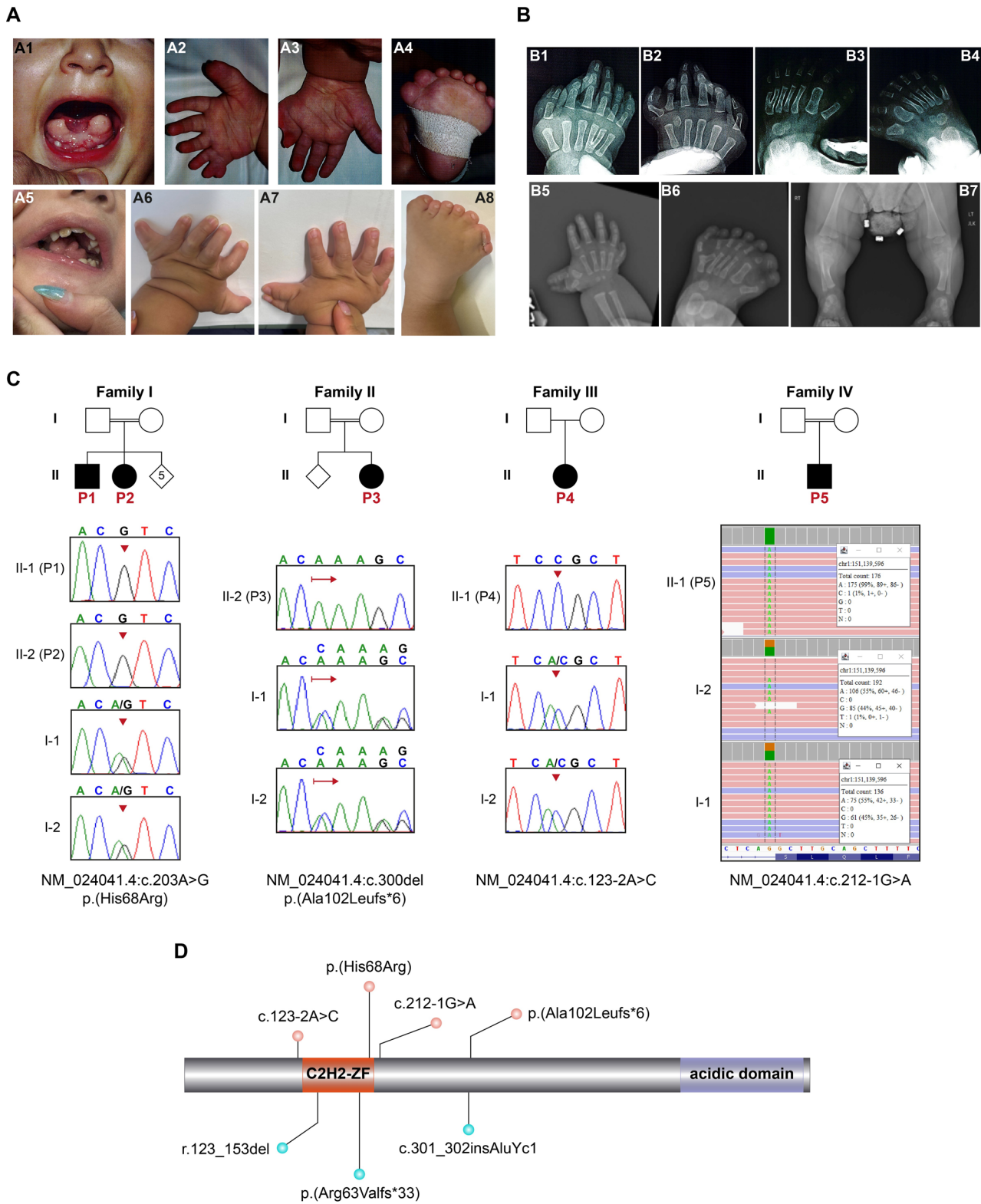


Fig. 1 (See legend on next page.)

(See figure on previous page.)

Fig. 1 Clinical and molecular findings in OFD syndrome-affected patients from this study. **A** Images of clinical features observed in P4 (A1-A4) and P5 (A5-A8). Oral cavity anomalies: lingual hamartoma (A1) and lobulated tongue as well as midline notching of the lower lip (A5). Skeletal defects: pre- and postaxial polydactyly of hands and feet (A2-A4, A6-A8). **B** X-rays of P4 (B1-B4) and P5 (B5-B7). Images show pre- and postaxial polydactyly of hands and feet, Y-shaped metacarpals/metatarsals (B1-B6), and bilateral tibial hemimelia (B7). **C** Family pedigrees and Sanger sequencing chromatograms or IGV scans from genomic DNA of P1-P5 and their parents showing the corresponding variants identified in *SCNM1*. **D** Schematic representation of the *SCNM1* protein illustrating the position of conserved functional domains and OFD syndrome-causing variants from this work (red) as well as those previously reported (blue)

according to clinical examination and parental saying. Intellectual disability was not measured by standardized tests. The patient has never been to school.

His younger affected sister (P2) presented with a similar phenotype. Prenatal ultrasound detected bilateral polydactyly of hands and feet. She was born at 38-week gestation with normal growth parameters (weight: 50th percentile, length: 50th percentile, OFC: 62nd percentile). Neonatal period was marked by Hirschsprung disease, which was treated by surgery. At age 4 years, she presented overweight (+3SD). She had abnormal pinna morphology, broad forehead, tongue hamartoma and gingival clefts. She had pre- and postaxial polydactyly of hands, bilateral preaxial polydactyly of feet, bilateral syndactyly between the 2nd and 3rd toes, and bifid thumbs and halluces. Cardiac investigations revealed bicuspid aortic valve. Brain MRI showed ventriculomegaly and cochleovestibular malformations. Abdominal ultrasound was normal. She had global developmental delay including speech delay, with first words pronounced at 1 year of age. Motor delay was noted but probably mainly due to skeletal malformations. She walked unaided at 18 months of age which is in the upper limit of the normal range. Neurological examination showed oculomotor apraxia, axial hypotonia and limb hypertonia. There was no history of seizures, and no features of autism spectrum disorder or other behavioral disorders.

Family II: The patient of family II (P3) is the second child of healthy first-cousin parents. Pregnancy and neonatal issues are unknown except that she underwent surgery for midgut volvulus with excision of a gangrenous ileum and caecum. At 13 years of age, she had midline notching of upper lip, bifid tongue, hamartoma of the tongue and hypodontia with missing lower central incisors. Digital features included bilateral pre and postaxial heptadactyly of hands and bilateral preaxial polydactyly of feet, bifid thumbs and syndactyly of 1st – 2nd and 6th – 7th fingers/toes. She has an equinovarus deformity and short tibia. No cardiac, renal or liver defects were detected. Brain MRI revealed prominent lateral ventricles. Presence of neurodevelopmental issues is uncertain. The family was lost to follow-up.

Family III: The patient of family III (P4) is a two-years-old female born to healthy and suspected consanguineous parents. Birth and childhood are not documented owing to the family's poor medical follow-up. She presented with hamartoma of the tongue and bilateral pre-,

post- and mesoaxial polydactyly of hands and feet (octodactyly and heptadactyly of hands, heptadactyly of feet) (Fig. 1A, B). She had talipes equinovarus of both feet. Craniofacial dysmorphism included broad nasal bridge, epicanthus, hypertelorism, thin lip vermilion and synophrys. Brain scan was suggestive of cerebral atrophy. She had global developmental delay including absence of language with independent walking at the age of 2 years. Neurodevelopmental tests were not performed.

Family IV: The affected child of family IV (P5) is a 2 years old male born at term to healthy consanguineous parents. The antenatal period was marked by mild polyhydramnios and bilateral clubfeet. Maternal prenatal vitamins were the only medication reported during pregnancy. At birth, he had normal growth parameters (weight: 23rd percentile, length: 35th percentile and OFC: 20th percentile), bilateral equinovarus deformity, bilateral pre- and postaxial polysyndactyly of hands and feet with bifid thumbs, micropenis, bilateral undescended testes, broad nasal bridge, cleft soft palate, lobulated tongue, midline notching of lower lip and micrognathia. X-rays revealed bilateral tibial hemimelia, supernumerary thoracic vertebrae and Y-shaped metatarsals (Fig. 1A, B). Cardiac investigation showed patent foramen ovale with clinically insignificant tiny left-to-right shunt, not requiring cardiac monitoring. Placement of a G-tube was necessary due to dysphagia and silent aspiration found on a swallow evaluation related to feeding difficulties. Brain MRI was normal. At 23 months of age, he had global developmental delay characterized by the absence of speech and walk, bilateral conductive hearing loss, and delayed gross and fine motor development. Neurodevelopmental tests were not performed. He has decreased tone of neck and trunk, and presented oculomotor apraxia.

Clinical characteristics of these patients are summarized in Table 1.

Genetic analysis

Quad exome sequencing in family I (P1, P2 and parents) identified a homozygous missense variant in *SCNM1* in P1 and P2 (NM_024041.4:c.203A>G, p.(His68Arg)). Both parents were heterozygotes for the same variant (Fig. 1C). The p.(His68Arg) variant involves a highly evolutionary conserved amino acid which is part of the C2H2 zinc finger (ZF) domain of *SCNM1* (Fig. 1D and Figure S1), and is predicted as damaging by in silico scores (SIFT:0;

PolyPhen-2:0.997; AlphaMissense:0.975). Patients from families II and III (P3 and P4) were analyzed by singleton exome sequencing. Deleterious variants in *SCNM1* were detected in both patients. P3 had a homozygous frameshift variant in *SCNM1* exon 4 (NM_024041.4:c.300del, p.(Ala102Leufs*6)), and P4 a homozygous splice-site variant eliminating the acceptor splice site of *SCNM1* intron 2 (NM_024041.4:c.123-2A>C) (TraP score:0.438, percentile 99%). The parents of P3 and P4 were confirmed to be heterozygous for the corresponding variant (Fig. 1C). The patient from family IV was analyzed by trio-based exome sequencing (P5 and parents). He was found to have a homozygous splice-site variant affecting the acceptor splice site of *SCNM1* intron 3 (NM_024041.4:c.212-1G>A) (TraP score:0.61, percentile 99%). This variant was present in his parents in the heterozygous state (Fig. 1C). Due to unavailability of samples for RNA extraction from P4 and P5, the impact of the splice-site variants identified in these individuals on the *SCNM1* mRNA could not be accurately determined. All variants detected in this study were absent or at very low frequency ($<1e-5$; with no homozygotes) in gnomAD (v4.1.0). Following American College of Medical Genetics (ACMG) recommendations, frameshift and splice-site variants from P3-P5 were classified as likely pathogenic (PVS1, PM2, PP4).

Functional validation of the *SCNM1* p.(His68Arg) variant

Pathogenicity of the p.(His68Arg) variant was investigated in dermal fibroblasts generated from a skin biopsy of P2. Immunoblot analysis showed the amount of *SCNM1* protein to be decreased by 62.78% in the cells from this patient with respect to control cells, while the levels of *SCNM1* mRNA quantified through RT-qPCR resulted to be similar in both, patient and control cultures (Fig. 2A, B). Next, we proceeded to assess *SCNM1* function in the fibroblasts from P2. To achieve this, we studied a set of U12-intron containing genes whose expression was previously reported to be decreased in the absence of *SCNM1* due to impaired processing of their U12 introns [3]. The result of this analysis showed that the abundance of the canonical transcripts of *TMEM107*, *CIBAR1*, *DERL2*, *ZC3H8* and *C17orf75* in the fibroblasts from P2 was reduced by 64.1%, 69.9%, 64.6%, 57% and 74.4%, respectively, in relation to control fibroblasts (Fig. 2C). In accordance with this, the fibroblasts from P2 were additionally characterized with diminished amount of *CIBAR1*, *DERL2*, *ZC3H8* and *C17orf75* proteins (Fig. 2D and Figure S2).

The presence of primary cilia alterations in the cells from P2 was determined through confocal immunofluorescence using the axonemal marker acetylated tubulin. In comparison to control cells, the fibroblasts from P2 had elongated cilia ($5.26 \pm 1.62 \mu\text{m}$ vs. $3.45 \pm 0.92 \mu\text{m}$

for C1 and $3.9 \pm 1.13 \mu\text{m}$ for C2) (Fig. 2E, F), and a slight reduction in the ciliation percentage ($74.59 \pm 5.47\%$ vs. $90.74 \pm 4.25\%$ for C1 and $94.36 \pm 2.93\%$ for C2) (Fig. 2G). These results are consistent with those previously reported in cells lacking *SCNM1* [3].

To further confirm the pathogenicity of the p.(His68Arg) amino acid change, we conducted phenotypic rescue experiments in *SCNM1* null fibroblasts (*SCNM1*^{-/-}) using a lentiviral system. Similar to what was previously reported [3], introduction of the *SCNM1* WT protein into *SCNM1*^{-/-} cells restored the expression of *TMEM107*, *CIBAR1*, *DERL2*, *ZC3H8* and *C17orf75*, both at the transcript and protein levels (Figure S3), as well as the ciliary defects associated with the loss of *SCNM1* (Figure S4). In contrast, lentiviral-mediated overexpression of the *SCNM1* protein harboring the p.His68Arg variant in *SCNM1*^{-/-} cultures caused no significant effects on any of the features associated with *SCNM1* deficiency (Figure S3 and S4).

Altogether, these results indicate that the p.(His68Arg) variant leads to a non-functional *SCNM1* protein. Accordingly, the p.(His68Arg) variant was classified as likely pathogenic (PS3, PM2, PM1, PP3, PP4, BP1).

Discussion

In this study, we describe five new patients from four unrelated families with an OFD syndrome phenotype caused by biallelic variants in *SCNM1*. This is the second report of patients with OFD syndrome due to likely pathogenic variants in this gene. The present work adds four new disease-causing variants to the molecular landscape of *SCNM1*, including a frameshift, two splice site and a missense variant (Fig. 1D). Here we have shown that the p.(His68Arg) variant has no effect at the mRNA level, but results in a reduced amount of protein, suggesting that this amino acid is important for *SCNM1* protein stability. His68 is one of the four invariant amino acids involved in zinc ion coordination characteristic of the C2H2 ZF structural motifs, and thus it is a critical residue for the molecular conformation of this domain. Previous work involving analysis of the cryo-EM structure of the purified human minor spliceosomal B^{act} complex, indicated that the C2H2 ZF domain of *SCNM1* interacts with the branch point site/U12 duplex and SF3b155, SF3b145, and CDC5L proteins [5]. Considering this, increased degradation of *SCNM1* due to abnormal protein folding and/or the disruption of *SCNM1* protein interactions is a possible mechanism that could explain the reduced amount of *SCNM1* protein observed in the fibroblasts from P2 carrying the p.His68Arg variant. Furthermore, we also demonstrated in this study that the phenotype of *SCNM1*^{-/-} cells was not rescued by overexpression of the *SCNM1*-His68Arg protein, indicating that this variant leads to a non-functional protein and highlighting

Table 1 Clinical features of *SCNM1* patients

Patients	Family I		Family II	Family III	Family IV
	P1	P2	P3	P4	P5
Sex	M	F	F	F	M
Country of origin or Ethnicity	Afghanistan	Afghanistan	India	Morocco	Hispanic
Consanguinity	+ (first cousin parents)	+ (first cousin parents)	+ (first cousin parents)	N/A (suspected)	+
Age at last examination	14 yo	4 yo	13 yo	6 yo	23 mo
weight (SD)	60.3 kg (+ 2 SD)	21.5 kg (+ 3 SD)	N/A	N/A	12.4 kg (0 SD)
length (SD)	149 cm (+ 1.5 SD)	104 cm (+ 0.05 SD)	N/A	N/A	76.5 cm (− 2 SD)
OFC (SD)	57 cm (+ 1 SD)	50 cm (0 SD)	N/A	N/A	46.8 cm (− 1.5 SD)
Cranio-facial					
Broad forehead	−	+	−	−	−
Eye anomalies	Right cataract	−	−	Epicanthus, Hypertelorism	N/A
Synophris	+	N/A	N/A	+	+
Nose anomalies	−	−	−	Broad nasal bridge	Broad nasal bridge
Ears anomalies	Low set ears	Abnormal pinna morphology	−	N/A	−
Mouth anomalies	Midline notching of upper lip	−	Midline notching of upper lip	Thin vermilion of the upper/lower lip	Midline notching of lower lip
Oral anomalies	High palate, Hamartoma of tongue	Gingival cleft, Hamartoma of tongue, Bifid tongue	Bifid tongue, Hamartoma of tongue, Hypodontia	Hamartoma of tongue	Cleft soft palate, Lobulated tongue
Other	Horizontal chin crease	−	−	Possible malar hypoplasia	Micrognathia
Hand					
Syndactyly	+	+ (bilateral)	+ (bilateral)	−	+ (bilateral)
Polydactyly	Suspected polydactyly	+ (pre and postaxial) Hexadactyly at right	+ (pre and postaxial) Bilateral heptadactyly	+ (pre, post and mesoaxial) Octodactyly at right, Heptadactyly at left	+ (pre and postaxial) Heptadactyly at right, Hexadactyly at left
Y-shaped metacarpals	N/A	N/A	N/A	+	−
Other	Large first phalanges of fingers	Bifid left thumb, Large right thumb	−	−	Bifid thumb
Feet					
Syndactyly	+	+ (bilateral)	+ (bilateral)	−	+
Polydactyly	Suspected polydactyly	+ (postaxial) Bilateral hexadactyly	+ (preaxial)	+ (pre, post and mesoaxial) Bilateral heptadactyly	+ (pre and postaxial) Bilateral heptadactyly
Equinovarus deformity	+	N/A	+	+	+
Y-shaped metatarsals	N/A	N/A	N/A	+	+
Other	Large first phalanges of toes	−	Bifid halluces, Congenital talipes	−	Bifid halluces
Systemic					
Cardiac anomalies	−	Bicuspid aortic valve	N/A	N/A	Patent foramen ovale, Left-to-right shunt
Gastrointestinal disturbance	−	Hirschsprung disease	N/A	N/A	G-tube
Skeletal anomalies	−	−	Mesomelic leg shortening	N/A	Mesomelic leg shortening, Short tibia
Neurodevelopmental					
Global developmental delay	+	+	N/A	+	+
Intellectual disability	+	N/A	N/A	N/A	N/A
Speech delay/impairment	+	+	N/A	+	+
Motor delay	+	+	N/A	+	+
Neurological					
Oculomotor apraxia	−	+	−	−	+

Table 1 (continued)

Patients	Family I		Family II	Family III	Family IV
	P1	P2	P3	P4	P5
Structural brain anomalies	–	Ventriculomegaly, Cochleovestibular malformations	Prominent lateral ventricles	Cerebral atrophy	–
Other	–	Axial hypotonia, Limb hypertonia	–	–	Bilateral conductive hearing loss, Silent aspiration, Micropenis, Undescended testes, Hypotonia

N/A: not available, SD: standard deviation (WHO growth chart reference), (–): Absent. (+): Present

the pivotal role of His68 in *SCNMI* function. In agreement with this, the fibroblasts from P2 were featured with defects in the expression of U12-intron containing genes and ciliary abnormalities equivalent to those previously described in fibroblasts from another patient homozygous for a loss-of-function variant in *SCNMI* [3]. Hence, until now, all nine affected individuals identified with *SCNMI* variants have homozygous loss-of-function variants: 3 frameshift, 2 splice-site, 1 splice-altering and 1 missense variant (p.(His68Arg)) (Fig. 1D).

Combining the patients of this study and those of the previous report [3] (Table S1), the *SCNMI*-associated phenotype includes mainly bilateral postaxial polydactyly of hands and feet (8/8, 100%), tongue hamartomas (8/9, 89%), foot syndactyly (8/9, 89%), broad nasal bridge (6/9, 67%), low-set ears (4/8, 50%), micro/retrognathia (5/8, 63%), horizontal chin crease (5/8, 63%), hypo/microdontia with missing incisors (5/7, 71%), arched/cleft palate (6/9, 67%), short limbs (5/7, 71%), talipes equinovarus (5/8, 63%), delayed speech (6/7, 86%) and various structural anomalies detected by brain MRI (4/8, 50%). Cardiac, gastrointestinal and genitourinary malformations were found in only a few numbers of patients. This phenotype appears highly suggestive of OFD type II, because of the association of polydactyly and Y-shaped metacarpal and the absence of kidney disorders. However, we also identified novel signs overlapping with other OFD subtypes including intellectual disability/global developmental delay, motor delay and speech delay. Overweight, which is part of the broad spectrum of ciliopathies, was noticed in two patients, and neurological abnormalities including oculomotor apraxia and/or hypo/hypertonia, were detected in two patients.

SCNMI-deficient cells exhibit aberrant splicing of targeted transcripts including ciliary genes such as *TMEM107* and *CIBARI*. *TMEM107* encodes a subunit of the MKS complex that appears essential for the recruitment of other subunits of the MKS module (MKS1, *TMEM17*, *TMEM237* and *TMEM231*) many of which, including *TMEM107*, are associated with OFD type VI syndrome. The MKS module is crucial for the transition zone of primary cilia, serving as a gate to ensure a specific ciliary protein composition. This kind

of OFD syndrome is mainly characterized by the presence of molar tooth sign on brain MRI, which is absent in *SCNMI*-patients, but also by neurological features including oculomotor apraxia and hypotonia. Intellectual disability and postaxial polydactyly are also frequently associated with OFD VI, and similarly, Y-shaped metacarpals/metatarsals are common in patients with this type of OFD, including *TMEM107*-mutated patients [6]. In the patients with *SCNMI* variants from this study, postaxial polydactyly and intellectual disability were constant but the molar tooth sign was absent, which ruled out OFD VI syndrome. However, there is a strong clinical overlap between the *SCNMI*- and the *TMEM107*/OFD VI phenotypes that is supported at the molecular level by the strong impact of *SCNMI* variants on *TMEM107* expression. In fact, as in the case of *SCNMI*-deficient cells, fibroblasts derived from patients with variants in *TMEM107* were described with impaired ciliogenesis and increased length of primary cilia [7]. Skeletal abnormalities like short limbs, which are present in around 60% of *SCNMI*-related patients, are not observed in OFD VI syndrome and are mostly frequent in OFD genes encoding centrosomal or basal bodies proteins such as *KIAA0753* or *NEK1*. In line with this, *CIBARI*, a basal body protein involved in primary cilium formation, and primarily associated with isolated postaxial polydactyly [8], is severely affected by the loss of *SCNMI* function. Of note, a patient carrying pathogenic variants in *CIBARI* was recently described with polydactyly and additional ciliopathic manifestations including polycystic kidneys and cerebellar vermis hypoplasia [9]. Likewise, the association of cardiac defects and deafness which is present in P5, is also observed in patients diagnosed with OFD VI due to variants in genes encoding the CPLANE complex located in the basal body (*INTU*, *WDPCP*) [10].

Conclusions

This study provides support for the involvement of *SCNMI* in OFD syndrome and increases the mutational landscape of this gene by adding four novel variants (one frameshift, two splice-site and one missense variant), leading to a total of seven causal *SCNMI* variants now reported. Additionally, we show that the *SCNMI*

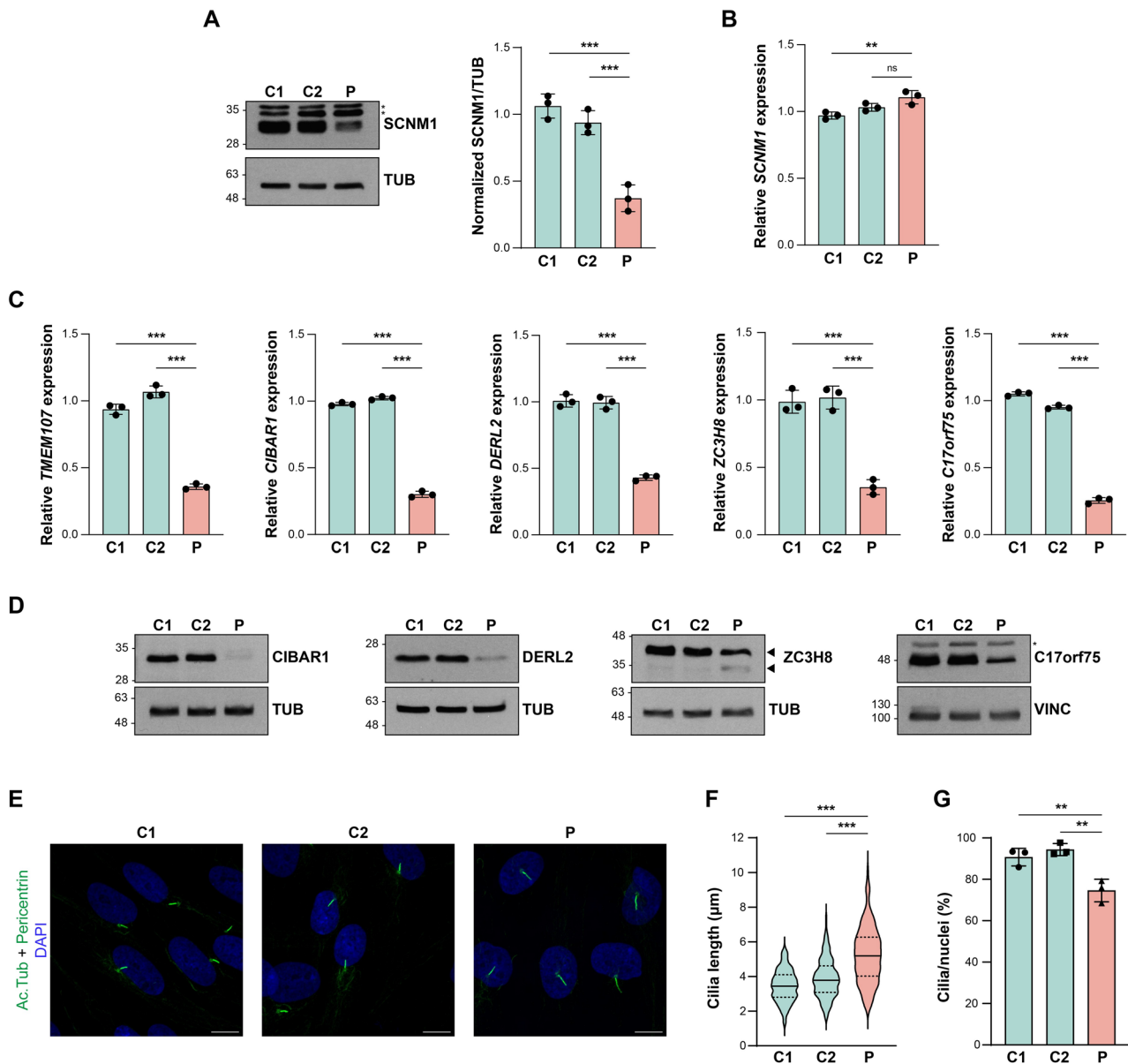


Fig. 2 Functional evaluation of the *SCN11* p.(His68Arg) variant. **A** Representative immunoblot of *SCN11* in fibroblasts from P2 (P) and controls (C1, C2). Tubulin (TUB) was used as loading control. Asterisks: non-specific bands. Right graph: densitometry analysis of *SCN11*/TUB ratio normalized to the mean value of control samples. $n = 3$. **B, C** Relative mRNA quantification of *SCN11* (**B**) and *TMEM107*, *CIBAR1*, *DERL2*, *ZC3H8* and *C17orf75* (**C**) by RT-qPCR in P and control fibroblasts. $n = 3$. Gene expression was normalized against the geometric mean of *GAPDH* and *GUSB* mRNA levels. The Δ Ct mean value of control fibroblasts (C1, C2) was used as calibrator to calculate $\Delta\Delta$ Ct. **(D)** Representative Western Blot images for *CIBAR1*, *DERL2*, *ZC3H8* and *C17orf75* in fibroblasts from P and controls. Loading controls: Tubulin (TUB) and vinculin (VINC). $n = 3$. Asterisk: non-specific band. For *ZC3H8*, the top arrowhead indicates the full-length protein and the lower arrowhead a shorter protein variant previously shown to be generated by an alternative splicing event induced by *SCN11* deficiency [3]. Densitometry analysis of these blots is provided in Figure S2. **E** Maximum intensity projection images of primary cilia from P and control fibroblasts obtained through confocal immunofluorescence illustrating longer cilia in P fibroblasts. Green: acetylated tubulin (axoneme) and pericentrin (basal body/centrosome). Blue: DAPI (nuclei). Scale bars: 10 μ m. **F** Cilia length measurements in fibroblasts from P and controls. At least 220 cilia from 3 independent biological replicates were measured in each type of fibroblasts. Median (solid line) and quartiles (dotted lines) are represented in violin plots. Differences in cilia length between control and P fibroblasts were analyzed by Kruskal-Wallis test with Dunn's multiple comparisons test. $***p < 0.001$. **G** Percentage of ciliated cells (cilia/nuclei) in P and control fibroblasts. For each type of fibroblasts, at least 252 cells from 3 independent biological replicates were analyzed. For A-C and G, graphs are expressed as mean \pm SD, and differences between control (C1 and C2) and P samples were assessed by One-way ANOVA with Šidák multiple comparisons test. $p > 0.05$: not significant (ns), $**p < 0.01$, $***p < 0.001$

associated clinical spectrum is broader, including global developmental delay/intellectual disability, oculomotor apraxia, deafness and skeletal defects, which were previously not reported. We conclude that the *SCNM1*-phenotype overlaps with that of the OFD II and OFD VI subtypes caused by variants in genes encoding proteins of the transition zone and/or centrosomal/basal body compartments. *SCNM1* appears as an OFD syndrome-causing gene which does not code for a ciliary protein, but regulates ciliary gene expression, thus, implicating defects in the minor spliceosome as a causative mechanism of ciliopathies.

Abbreviations

OFD	Oral-facial-digital
MRI	Magnetic resonance imaging
ZF	Zinc finger

Supplementary Information

The online version contains supplementary material available at <https://doi.org/10.1186/s40246-025-00868-v>.

Supplementary Material 1.

Acknowledgements

We are grateful to the patients and their families for their participation in this study. We thank the Centre de Calcul de l'Université de Bourgogne (CCuB) for the technical support and management of the informatics platform. This article resulted in part from a successful GeneMatcher match [11].

Author contributions

Conceptualization: ALB, VLRP; Methodology: AI. Data Analysis: AI, ALB, FTMT, IMW; Clinical investigation: AV, AP, DDS, LPS, KJ, JU, EA; Funding: VLRP, CTR; Supervision: VLRP, ALB; Writing original draft: ALB, VLRP; Writing review and editing: AI, VLRP, ALB. All authors read and approved the final manuscript.

Funding

A part of this work was supported by PID2022-139565OB-I00 funded by MCIN/AEI/10.13039/501100011033/FEDER/UE.

Data availability

Data supporting this manuscript is provided within the manuscript and supplementary information. Any other data not compromising patient confidentiality is available from the corresponding authors under reasonable request.

Declarations

Ethics approval and consent to participate

The studies involving human participants were reviewed and approved by the appropriate institutional review board of Dijon University Hospital. Patient fibroblasts were obtained through protocols approved by CHU Robert Debre/Hôpitaux de Paris. Functional studies in primary fibroblasts were approved by the Ethics Committees of Hospital La Paz (PI-6270) and CSIC. Informed consent was provided by all participants.

Consent for publication

Written informed consent was obtained from the patient(s), and minor(s) legal guardian/next of kin, for the publication of any potentially identifiable images or data included in this article.

Competing interests

IMW is an employee of and may own stock in GeneDx.

Author details

¹Instituto de Investigaciones Biomédicas Sols-Morreale (IIBM), Consejo Superior de Investigaciones Científicas-Universidad Autónoma de Madrid, Madrid 28029, Spain

²CIBER de Enfermedades Raras, Instituto de Salud Carlos III, Madrid 28029, Spain

³Université Bourgogne Europe, CHU Dijon Bourgogne, Laboratoire de Génétique Médicale, Centre Neomics, FHU-TRANSLAD, Centre de recherche Translationnelle en Médecine moléculaire, Dijon 21000, France

⁴INSERM-Université Bourgogne Europe-UMR1231, GAD, Dijon 21000, France

⁵Department of Genetics, AP-HP-Hôpital Robert Debré, Université Paris Cité Medical School, INSERM UMR 1141 "NeuroDiderot", Paris, France

⁶Department of Physiology, Faculty of Medicine, University of Kelaniya, Ragama, Sri Lanka

⁷GeneDx, LLC, Gaithersburg, MD 20877, USA

⁸Department of Pediatrics, Hayward Genetics Center, Tulane University School of Medicine, New Orleans, LA, USA

⁹Department of Human Genetics, Medical Research Institute, Alexandria University, Alexandria, Egypt

¹⁰CRMR Anomalies du Développement et Syndromes Malformatifs, Centre de Génétique, FHU-TRANSLAD, CHU Dijon Bourgogne, Dijon, France

¹¹Instituto de Genética Médica y Molecular (INGEMM), Hospital Universitario La Paz-IdiPAZ, ITHACA-ERN, Madrid 28046, Spain

Received: 24 July 2025 / Accepted: 9 November 2025

Published online: 25 November 2025

References

- Bruel AL, Franco B, Duffourd Y, Thevenon J, Jegou L, Lopez E, Deleuze JF, Doummar D, Giles RH, Johnson CA, et al. Fifteen years of research on oral-facial-digital syndromes: from 1 to 16 causal genes. *J Med Genet.* 2017;54:371–80.
- Ferrante MI, Giorgio G, Feather SA, Bulfone A, Wright V, Ghiani M, Selicorni A, Gamaro L, Scolari F, Woolf AS, et al. Identification of the gene for oral-facial-digital type I syndrome. *Am J Hum Genet.* 2001;68:569–76.
- Iturrate A, Rivera-Barahona A, Flores CL, Otaify GA, Elhossini R, Perez-Sanz ML, Nevado J, Tenorio-Castano J, Trivino JC, Garcia-Gonzalo FR, et al. Mutations in *SCNM1* cause orofacioidigital syndrome due to minor intron splicing defects affecting primary cilia. *Am J Hum Genet.* 2022;109:1828–49.
- Nishimura K, Yamazaki H, Zang W, Inoue D. Dysregulated minor intron splicing in cancer. *Cancer Sci.* 2022;113:2934–42.
- Bai R, Wan R, Wang L, Xu K, Zhang Q, Lei J, et al. Structure of the activated human minor spliceosome. *Science.* 2021. 371:eabg0879. <https://doi.org/10.1126/science.abg0879>.
- Chinen Y, Nakamura S, Yanagi K, Kaneshi T, Goya H, Yoshida T, Satou K, Kaname T, Naritomi K, Nakanishi K. Additional findings of tibial dysplasia in a male with orofacioidigital syndrome type XVI. *Hum Genome Var.* 2022;9:9.
- Shylo NA, Christopher KJ, Iglesias A, Daluiski A, Weatherbee SD. *TMEM107* is a critical regulator of ciliary protein composition and is mutated in orofacioidigital syndrome. *Hum Mutat.* 2016;37:155–9.
- Schrauwen I, Giese AP, Aziz A, Lafont DT, Chakchouk I, Santos-Cortez RLP, Lee K, Acharya A, Khan FS, Ullah A, et al. *FAM92A* underlies nonsyndromic postaxial polydactyly in humans and an abnormal limb and digit skeletal phenotype in mice. *J Bone Min Res.* 2019;34:375–86.
- EI-Dessouky SH, Sharaf-Eldin WE, Aboulgar MM, Mousa HA, Zaki MS, Maroofian R, Senousy SM, Eid MM, Gaafar HM, Ebrashy A, et al. Integrating prenatal exome sequencing and ultrasonographic fetal phenotyping for assessment of congenital malformations: high molecular diagnostic yield and novel phenotypic expansions in a consanguineous cohort. *Clin Genet.* 2025;108:33–48.
- Toriyama M, Lee C, Taylor SP, Duran I, Cohn DH, Bruel AL, Tabler JM, Drew K, Kelly MR, Kim S, et al. The ciliopathy-associated *CPLANE* proteins direct basal body recruitment of intraflagellar transport machinery. *Nat Genet.* 2016;48:648–56.

11. Sobreira N, Schietecatte F, Valle D, Hamosh A. GeneMatcher: a matching tool for connecting investigators with an interest in the same gene. *Hum Mutat.* 2015;36:928–30.

Publisher's note

Springer Nature remains neutral with regard to jurisdictional claims in published maps and institutional affiliations.